# Direct-Write Patterning of Biomimetic Lipid Membranes In Situ with FluidFM

Eider Berganza* and Michael Hirtz

ABSTRACT: The creation of biologically inspired artificial membranes on substrates with custom size and in close proximity to each other not only provides a platform to study biological processes in a simplified manner, but they also constitute building blocks for chemical or biological sensors integrated in microfluidic devices. Scanning probe lithography tools such as dip pen nano lithography (DPN) have opened a new paradigm in this regard, although they possess some inherent drawbacks like the need to operate in air environment or the limited choice of lipids that can be patterned. In this work, we propose the use of the fluid force microscopy (FluidFM) technology to fabricate biomimetic membranes without losing the multiplexing capability of DPN but gaining flexibility in lipid inks and patterning environment. We shed light on the driving mechanisms of the FluidFM mediated lithography processes in air and liquid. The obtained results should prompt the creation of more realistic biomimetic membranes with arbitrary complex phospholipid mixtures, cholesterol, and potential functional membrane proteins directly patterned in physiological environment.

KEYWORDS: *supported lipid membranes, SLB, biomimetic membranes, FluidFM, scanning probe lithography, SPL*
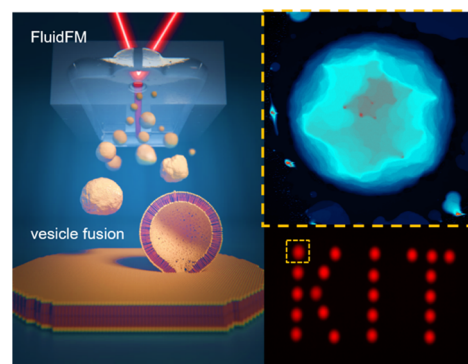
1. INTRODUCTION

Advances in nanotechnology have supported unprecedented understanding of mechanisms occurring in living cells, such as transport of molecules and ions across cell membranes, detection of signals in cell communication,[1] cell mechanics,[2] and functionality of different proteins.[3,4] Sophisticated nano scale fabrication tools, as well as high resolution character ization devices, have endowed the scientific community with the capability not only to study natural cells but also to mimic their behavior through the creation of artificial in vitro models allowing us to study their fundamental properties in a simplified manner.

In this context, supported lipid bilayers (SLBs) with many applications, e.g., in biosensing,[5,6] device functionalization,[7,8] drug screening,[9] as a DNA anchor,[10] capture of extracellular vesicles,[11] and so on, constitute a very active area of research in synthetic biology.[12−15] The fabrication of these biomimetic membranes is most commonly carried out by vesicle fusion based techniques, but these offer only limited control over the patterning process. Especially, site specific targeting, high resolution, and multiplexing capabilities (having more than one membrane constitution in a surface pattern at the same time) are not achieved through this method. Furthermore, the implementation of physiological conditions to preserve membrane proteins and exosomes[16−18] (nanosized vesicles excreted by cells) in their natural environment—where their correct function is guaranteed—still constitutes an obstacle that needs to be overcome.[19,20]

Maskless lithography techniques like dip pen nanolithog raphy with phospholipids (L DPN),[21] micropipette based approaches,[22] microchannel cantilever spotting (µCP),[23] microcontact printing (µCP),[24] and polymer pen lithography (PPL) with phospholipids[25] have all shown different strengths and weaknesses for the deposition of patterned SLBs in regard to resolution, throughput, and feasible compositions. When it comes to high resolution and multiplexing, L DPN stands out. This atomic force microscopy (AFM) setup based approach allows depositing nanosized elements with spatial resolution below 100 nm by transferring phospholipid inks adsorbed on the AFM tip through a water meniscus onto the desired substrate.[26] In addition to the high resolution, the technique can write multiple different compounds in parallel and within the same subcellular sized micropatterns (real multiplexing).[27]

However, L DPN struggles with creating membranes of realistic composition for phospholipid mixture and protein content due to inherent limitations. Its major drawback is that
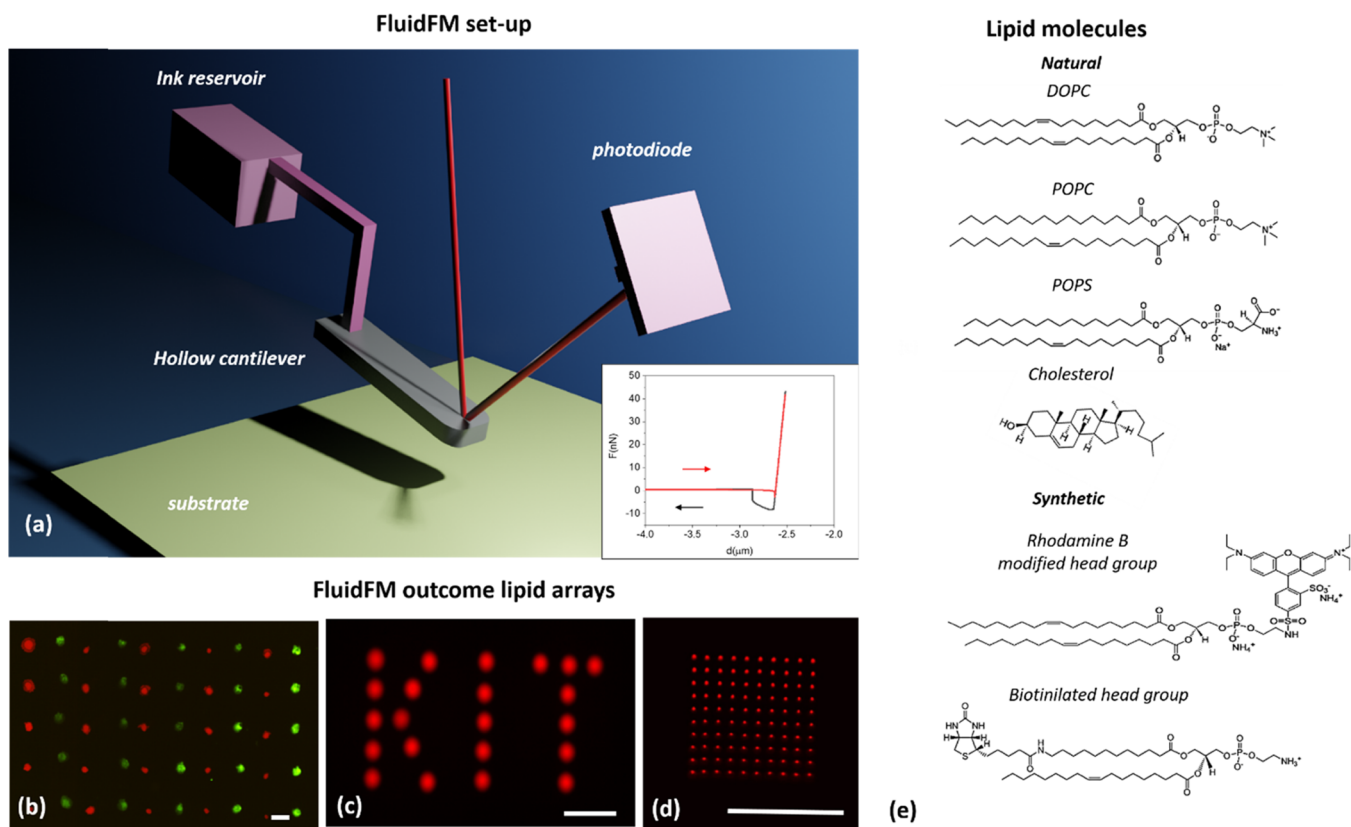
Figure 1. (a) Scheme of the FluidFM setup for patterning phospholipid inks. The inset shows a typical force−distance AFM curve used for force feedback control during patterning. (b) Fluorescence image (combined FITC/Texas red channels) of a multiplexed lipid array deposited by FluidFM. (c) KIT logo patterned with FluidFM, showing big spatial control capability. (d) High resolution lipid printing, showing an array of 10 × 10 features of approx. 1 μm diameter. (e) Lipid molecules integrated in the inks used in the experiments. Scale bars equal 100 μm.

it is generally performed in air (despite some isolated attempts in the past to directly implement lithography in liquid,[28] which poses complications in processing and makes its wide adoption not feasible). This means that the obtained phospholipid membranes are inverted compared to biological membranes ("tails out", facing the hydrocarbon chains outward of the membrane) and thus have to rearrange to their natural configuration ("heads out", facing the phosphate/glycerol headgroups outward of the membrane) during immersion in liquid for use in biological experiments.[29,30]

Generally, 1,2 dioleoyl *sn* glycero 3 phosphocholine (DOPC), an unsaturated phospholipid with a well adjusted humidity dependent behavior during the L DPN process, acts as a carrier ink.[8,21,31,32] While other phospholipids can be admixed to the DOPC to achieve specific functionality (e.g., as binding sites, model allergens, or fluorescent markers) or to obtain a more natural membrane composition, these admixings are limited to a few mol % (depending on the specific addition) before altering the writing behavior to an extent prohibiting patterning via L DPN.[27,33]

Recently, fluid force microscopy (FluidFM) has emerged as a scanning probe lithography (SPL) technique that combines the accuracy of force control positioning and the versatility of microfluidics.[34,35] A microsized channel patterned in an AFM cantilever creates a closed fluidic channel that allows dispensing locally any chosen solution, while the applied force with the tip is controlled through a standard AFM laser detection system. As the FluidFM technology develops,[36] many groups have started to harness the new perspectives

opened by it, from fluorescently labeled dye injection into cell nuclei[37] to electrochemical patterning by dispensing of the electroactive species with high precision.[38]

To the best of our knowledge, in the work presented here, we employ the FluidFM technology for the first time in the creation of lipid patches, demonstrating the particular favorable properties of this approach. This opens up new possibilities for the creation of more realistic biomimetic membranes and extends the capabilities of the other described soft lithography techniques toward this cause. In particular, the FluidFM can work as an alternative tool to fabricate functional supported lipid biomimetic membranes, overcoming the described inherent limitations of L DPN, without losing its multiplexing capability.

2. MATERIALS AND METHODS

2.1. Preparation of Phospholipid Inks. The phospholipids, dissolved in a chloroform solution, were purchased from Avanti Polar Lipids. For most of the experiments, 1,2 dioleoyl *sn* glycero 3 phosphocholine (DOPC) was used as a model ink, with 1 mol % fluorescently labeled Liss Rhod, to conduct to make it visible for a fluorescence microscope. For some experiments, biotinylated Biotinyl Cap PE was added to DOPC to obtain a concentration of 5 mol %. To prevent degradation of the FluidFM probe microfluidic channels, chloroform was evaporated in a desiccator and then the lipids were resuspended in DI water. The new ink was sonicated for at least half an hour to ensure good mixing and to obtain small vesicles below 50 nm. Finally, 25% volume of glycerol was added to the phospholipid ink to increase the boiling point of the ink and prevent its evaporation during the experiments. All other chemicals were obtained from Sigma Aldrich (Germany) and used as received.

2.2. Preparation of Substrates and Contact Angle Measurements. Generally, glass substrates were cleaned through a standard procedure, by sonication in acetone, ethanol, and DI water subsequently. To study the influence of the different substrates over the patterning shape and printed area, (1) a hydrophilic substrate was prepared by the standard cleaning procedure and subsequent exposure to 5 min of oxygen plasma (200 W, 50 sccm oxygen flow, in an Atto system Diener Electronics, Germany) and (2) hydrophobic substrates were prepared by cleaning the glass substrate, 5 min of exposure to oxygen plasma, (i) immersion into (3 glycidyloxypropyl) trimethoxysilan (GPTMS) (2 vol % in toluene) for 4 h or, alternatively, (ii) immersion into 7 octenyltrimethoxysilane (10 vol %) for 24 h and then washing through the standard procedure again. The substrate hydrophilicity was then characterized through contact angle measurements, by depositing a 2 μL water droplet onto bare functionalized substrates at room temperature using an OCA 20 contact angle analyzer (Dataphysics, Germany).

2.3. FluidFM Nanolithography. The lipid writing was performed using a FluidFM system from Nanosurf (Switzerland). Most experiments were performed with a FluidFM micropipette (Cyto surge, Switzerland), a tipless cantilever with an aperture of 8 μm at the end, and a force constant of 2 N/m. For smaller patch patterning, a nanopipette (Cytosurge, Switzerland) was chosen, with an aperture of 300 nm at the end of the tip and the same force constant. The probe reservoir was loaded with 5 μL of ink before the experiments. Before starting the experiments, a pressure of 1000 mbar needs to be applied to fill the microchannels with ink. To perform the patterning in the desired area, the spotting option of the Cytosurge software is used and the desired applied force, pressure, and pulse duration parameters are chosen. The maximum area that can be patterned at once enabling the force feedback control is 100 × 100 μm^2 (corresponding to the maximum scan range of the AFM head). After patterning in air, the water and glycerol solvent spontaneously evaporate within a few seconds. To ensure that the lipid patches are stable, characterization measurements are performed 1 day after the sample fabrication. For patterning in liquid, a 200 μL DI water droplet is placed on the substrate and a 30 μL water droplet is placed on the FluidFM probe. When the scan head is mounted on the stage, a good water meniscus needs to be achieved between the probe and substrate. After lithography, no special treatment is needed.

2.4. Fluorescence Imaging. Fluorescence microscopy images were obtained on a SARFUS 3D AIR microscope from Nanolane (France) with onboard software Sarfusoft (Nanolane). The rhod amine compatible Filter Set 71 (Zeiss, Germany) was used as a light filter and a green fluorescent protein (GFP) compatible filter was used for the biotin streptavidin binding experiment visualization.

2.5. Atomic Force Microscopy Imaging. AFM images were performed on a Dimension Icon system (Bruker, Germany). Measurements in air were done in amplitude modulation with PPP NCHR model probes from Nanosensors (Switzerland), setting a typical oscillation amplitude of 10 nm. The volumes were quantified through careful data analysis and using the flooding option of the WSxM software. Measurements in water were performed with a soft AFM cantilever tip (PNP TR Au 20 model) from NanoWorld (Switzerland).

2.6. Biotin-Streptavidin Binding Experiments. To prevent nonspecific binding, the samples were incubated in a 10% bovine serum albumin (BSA) solution from Sigma Aldrich (Germany) for 15 min. Subsequently, the BSA solution was removed and the sample was washed several times. The sample was then incubated for 15 min with a 1:200 streptavidin cy3 solution (Sigma Aldrich, Germany) in phosphate buffered saline (PBS) and washed again.

All procedures were done at room temperature.

3. RESULTS

3.1. FluidFM with Lipids. A schematic of the FluidFM setup is presented in Figure 1a. A tipless cantilever with an internal microchannel mounted on an AFM setup allows dispensing the prepared phospholipid ink with very high spatial control onto the desired areas of the substrate. The system is equipped with a force feedback control (laser and photodiode) to ensure controlled tip−substrate contact during deposition with nanonewton range force, avoiding damage to soft substrates. A typical force−distance curve plotted before the lithography process is shown in the inset.

While in classic L DPN, phospholipids are written solvent free after coating of the DPN tip, in our approach, to allow proper ink flow in the FluidFM microfluidic system, water based ink formulations were used. In such aqueous environ ments, the phospholipids arrange as vesicles.[39,42] A small amount of glycerol (20 vol %) is generally added to the prepared ink to prevent evaporation and avoid tip clogging problems, particularly when working in air. The ink is then loaded into the reservoir and the lithography process is triggered by applying positive pressure to the ink reservoir connected to the microchannel.

Typical outcomes of FluidFM lithography with phospholipid inks are displayed in Figure 1b−d. In contrast to classical vesicle fusion methods to obtain biomimetic phospholipid membranes,[2] it becomes immediately obvious that a high spatial control over the patterned dot array is possible and even multiplexing can be achieved. Although most of the results presented in this manuscript are aiming at the 10−100 μm range (being the most adequate size for many applications), for obtaining smaller features, different FluidFM probes can be used. Lipid dots of a few tens of microns of diameter (as in Figure 1b,c) were obtained using a tipless cantilever with an 8 μm aperture, while cantilevers with hollow tips and nanometer range aperture at its end were used for patterns of smaller diameter features, as shown in Figure 1d. In this case, the process is governed by the high capillary force, as a result of the narrow dimensions of the inner channel, which gives rise to a stamping like transfer of the ink molecules to the substrate. AFM characterization of small lipid dots can be found in Supporting Information 1.

Notice that most of the systematic studies presented in this work have been carried out utilizing a water based ink solution with fluorescently labeled DOPC vesicles. All lipid molecules used along the different experiments are summarized in Figure 1e.

The next sections encompass a detailed study of the lithography processes in air and liquid media, focusing on how the experimental parameters, namely, applied pressure to the reservoir and the duration of this pressure pulse, affect the final feature size and impact the two lithography modes.

3.2. Lithography in Air Environment. *3.2.1. Determination of Threshold Pressure.* Preliminary attempts to print a DOPC vesicle ink revealed that there is a certain threshold pressure value beyond which patterning is not possible. This value is related to the resistance to expel the fluid out of the cantilever aperture. In general terms, the ink flow is affected by both the hydrodynamic resistance of the microchannel and the aperture. However, the influence of the microchannel is negligible in comparison to the aperture when operating in air environment, where the liquid−air interface at the aperture yields a high surface tension needing to be overcome for successful printing. For different used inks, the threshold pressure value to achieve printability varies according to its physicochemical characteristics. To demonstrate that the FluidFM technology is extensible to the patterning of lipids and mixtures of different characteristics, different inks were trialed and their threshold pressure value was determined. In

Section 2 of the Supporting Information, we exemplify the procedure followed to calculate the threshold pressure using our model ink DOPC to be 24 mbar.

The obtained threshold values are compared to those of deionized water and a water/glycerol (80:20 vol %) mixture, which is used as a carrier in all of the lipid inks (Figure 2). The
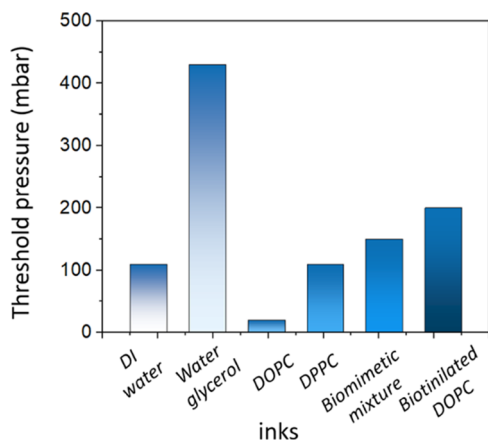
Figure 2. Threshold pressure values for inks with different types of phospholipid vesicles and pure solvents. All inks are mixed with 20 vol % glycerol to hinder evaporation.

addition of glycerol to the mixtures is needed to avoid premature evaporation of the ink when patterning in air, resulting in clogging of the microchannel. The results evidence that the water/glycerol mixture possesses the highest threshold pressure value and that the addition of different lipids lowers the pressure that we need to apply during the lithography process.

The success in writing a complex mixture of lipids constitutes a big step forward in the fabrication of biomimetic membranes via SPL methods. It is important to stress here that in other SPL and soft lithography methods, fluidity as well as specific physicochemical properties are key for smooth tip–substrate molecular transfer. In fact, since L DPN requires dipping the probe into the fluid state phospholipid ink, any phospholipid with gel–liquid transition above room temperature is challenging to pattern. In contrast, in the FluidFM approach, a water based ink is used, where the desired phospholipid mixture is suspended as vesicles. As the printing of these vesicle inks is not relying on phase state, remaining differences in surface tension of the inks can easily be addressed dynamically by applying matching pressures. Therefore, arbitrary and complex phospholipid mixtures that more realistically mimic real biomembranes can be patterned with high spatial control.

3.2.2. Writing Mechanism. Unveiling the mechanisms behind the lithographic process with the vesicle inks is important to have full control over the lipid membrane stack writing for features with customized size and shape. With this purpose in mind, the writing parameters, namely, working pressure and pulse length, have been assessed. Most applications of biomimetic membranes require patch sizes in the order of square micrometers; therefore, we focused our experiments on a tipless cantilever with an 8 μm aperture.

In the following systematic experiments elucidating the role of working pressure and pulse time, a water based ink containing DOPC vesicles labeled with 1,2 dioleoyl *sn* glycero 3 phosphoethanolamine N (lissamine rhodamine B

sulfonyl) (Rho PE) was used as a model. First, the pressure during writing of the features was varied while pulse time was fixed. For the series of patches displayed in Figure 3a, the pulse time was set to 250 ms and the pressure was increased up to 400 mbar. As it becomes obvious from the fluorescence microscopy images, the size of the patches increases with rising pressure in an applied pulse, which acts as a driving force to expel the ink droplet out of the tip aperture. Choosing a too small pulse time might lead to irregularities, resulting in different patches patterned at the same nominal writing conditions.

Further experiments were conducted with a longer pulse time. The lipid flow and the resulting feature area on the substrate can be fitted by a linear relation (Figure 3c,d). It should be noted here that the calculated flow is the pure lipid flow as extracted from the feature volume measured by AFM (an illustrative example is shown in Figure 3b), which differs from the total ink flow, where water constitutes the main part. Deviations from the linear curve can arise, especially at higher pressure values.

Previous studies of self assembled molecular structures conducted with other soft lithography techniques demonstrated that, while the feature volume is dependent on the specific fabrication parameters, the area or shape of the feature depends purely on its rearrangement as a result of its surface energy on the substrate.[30] A study on glass substrates with different functionalizations is included in Section 3 in the Supporting Information. Interestingly, on plasma cleaned substrates with zero water contact angle surfaces, the lipid dots keep a very high aspect ratio and do not spread—contrary to that expected in L DPN pointing to the different writing modalities for FluidFM. In contrast, on highly hydrophobic substrates, the lipids tend to spread as a result of the formation of inverse lipid bilayers. Figure 3d shows that the feature area also follows a linear trend. Further data lead to the conclusion that smaller feature volumes (<500 fl) result in a patch with a shape closer to a truncated cone, caused by rearrangement in the initially deposited ink droplet, while for volumes higher than 500 fl, the phospholipid spreading becomes more important, yielding more cylindrically shaped features. A detailed discussion of this effect is included in Section 4 in the Supporting Information.

To elucidate the effect of the pulse length on the process, several experiments were carried out setting a constant pressure of 30 mbar while varying the pulse time (Figure 3e,f). As intuitively expected, longer pressure pulses allow dispensing a larger volume of ink. The dependency of the feature volume with pulse length is, as in the case of pressure, also linear (Figure 3a), although here two differentiated regimes are observed. In the first regime, at a smaller pulse length, smaller feature sizes are achieved, but size increases at a steeper slope. In the second regime, at longer pulses (>1 s), the slope of the line decreases. The switch between the two regimes takes place once the available free volume between cantilever and substrate is filled, and the additional resistance to displace the ink now trapped below the cantilever is slowing down the ink deposition. Geometrical calculations yield an estimated available volume of ~1800 fl below the cantilever. The experimentally obtained value for the change in regime is around 100 fl, which is an order of magnitude lower because it represents the amount of remaining phospholipid, which should be considerably smaller than the overall volume of the dispensed ink.
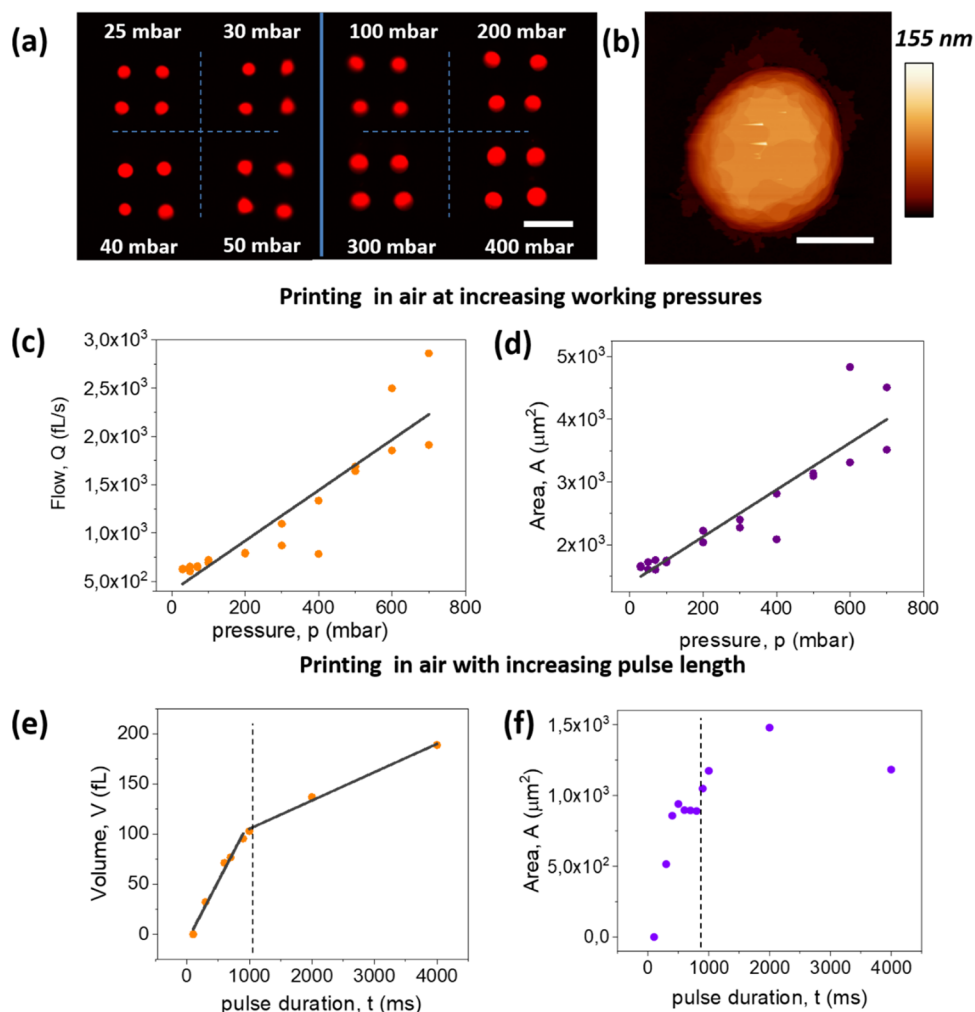
Figure 3. Effect of working pressure and pulse length over the patch size for lithography in air environment. (a) Typical fluorescence microscopy images of an experiment of lipid printing at increasing working pressure and a pulse length of 250 ms. Scale bar equals 50 μm. (b) AFM image of a lipid dot topography. Scale bar equals 10 μm. (c) Linear behavior of lipid flow and (d) feature area vs applied pressure. (e) Volume and (f) area of the lipid dots increase monotonically with pulse length.

3.3. Lithography in Liquid Environment. Implementation of patterning processes for bioactive surfaces directly in liquid environment is highly desirable because it allows fabrication in an environment optimal for biological substances, where the functionality of the patterned specimens is not compromised. In the specific case of biomimetic membranes, this feature is of great importance, for instance, to add functional proteins as it prevents denaturation or other nondesirable effects. Patterning directly in liquid also helps to keep more accurate control over the phospholipid stacks, as the phospholipid membranes necessarily rearrange, often deteriorating feature shapes, when they are transferred from air to liquid.[29,30]

When the cantilever is immersed in liquid with the vesicle ink loaded and a small overpressure is applied to the reservoir, the vesicles exit the aperture, diffusing through the aqueous medium. When the vesicles reach the substrate surface, they can fuse, forming circular lipid patches (Figure 4).

To elucidate the dependence of the lipid transfer and feature size on the writing parameters in liquid, several features were fabricated at increasing working pressures and pulse lengths, with the DOPC/Rho PE vesicle ink in deionized water. Strikingly, AFM measurements reveal that here, in all cases, a

single bilayer of phospholipids was formed (the thickness of one DOPC bilayer in aqueous media is known to be about 6 nm),[60] regardless of the writing parameters. Figure 4d displays representative AFM images obtained in liquid with their corresponding profiles (more details and additional AFM measurements are given in Section 5 in the Supporting Information). As the patterning is carried out in the presence of water, the strong hydrophobic forces between the hydrocarbon chains lead to vesicle fusion based writing mode yielding a single bilayer, which spreads on the substrate.[40,41] The obtained SLBs are very stable, and samples could be stored for days without deterioration of the lipid patches as long as they were kept in aqueous environment.

Since all of the patches present the same thickness, we focus on the effect of writing parameters on the patch area. In comparison to the lithography process in air, the resulting features are much more uniform and display a high homogeneity (Figure 4a,b), except for the lowest pressure or pulse length values, where the instrument error is higher. In fact, when working in liquid media, the lipid patch area sizes adjust much better to a linear behavior. This is a very clear asset of printing directly in liquid compared to lithography in air, where the patch size and shape are more prone to some
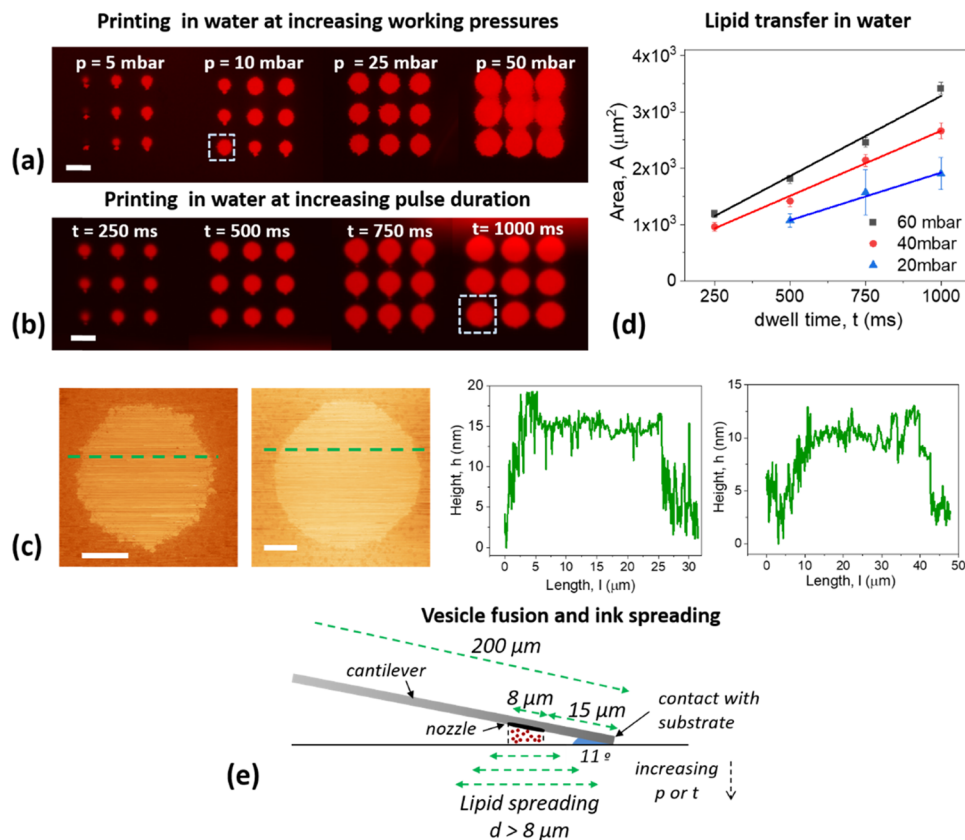
Figure 4. (a) Fluorescence microscopy image of a sequence of lipid patch prints at increasing pressure with a pulse length of 500 ms and (b) increasing pulse length and pressure fixed at 50 mbar. Scale bars equal 40 μm. (c) Linear dependence of the size of the patterned lipid patch on the pulse length for different applied pressures. Scale bars equal 10 μm. (d) AFM images in liquid of the lipid patches inside a frame in (a) and (b), with their corresponding profiles, showing a height indicative of a single bilayer. (e) Schematic explanation of the patterning process in water and the subsequent lipid spreading.

random fluctuations. In liquid, the printed lipid stacks are considerably more homogeneous.

When a pressure pulse is applied in liquid media, a vesicle cloud is ejected from the nozzle with a certain momentum toward the substrate where the vesicles fuse initially with the naked substrate and then with the already deposited parts of the bilayer, leading to spreading of the bilayer. The process can be characterized by a lateral diffusion constant as obtained from a linear fit of the data (see Figure 4c and Table 1). Higher

Table 1. Calculated Diffusion Coefficients from Experimental Data Displayed in Figure 4d

working pressure p [mbar]	diffusion coefficient D [m^2/s]
20	1.69×10^{-6}
40	2.31×10^{-6}
60	2.84×10^{-6}

pulse pressures yield bigger cloud formation and higher momentum of vesicles, thereby increasing also the apparent lateral diffusion coefficient. However, further experiments given in Section 6 in the Supporting Information show that the spreading of the patches depends on the solvent used as the printing environment.

Interestingly, despite the diffusion based printing mechanism and larger aperture (8 μm diameter), even smaller biomimetic membranes at sizes about 1×1 μm^2 can be obtained by implementing an alternative fabrication method.

Here, smaller lipid patches of rectangular shape could be achieved by first blocking the probe aperture with an air bubble and then printing by transferring self assembled phospholipids from the cantilever apex to the substrate in a stamping like mechanism (for details, see Section 7 in the Supporting Information).

4. DISCUSSION

4.1. Printing in Air versus Printing in Water. Experiments show that the lithography processes in air and liquid media differ significantly and lead to different outcomes for the membrane structure. The schematic representations of both processes are displayed in Figure 5.

In air environment, an ink droplet is pushed out of a tipless cantilever (Figure 5a) as a result of the positive applied pressure. The probe/surface contact facilitates the ink transfer. Upon contact, the droplet is squeezed between the cantilever and the substrate. When the probe is withdrawn, the droplet snatches off and the vesicles within the ink droplet fuse and arrange in three dimensional bilayer stacks, while water evaporates (Figure 5b).

Finally, the lipids rearrange according to their surface energy on the substrate (Figure 5c). The created lipid patches are fairly big, with diameters in the range of 10−100 μm and heights up to a few hundreds of nanometers. Conversely, if the fabrication is carried out in liquid environment, the vesicles are released through the probe aperture when positive pressure is applied (Figure 5d). They diffuse through the liquid and the
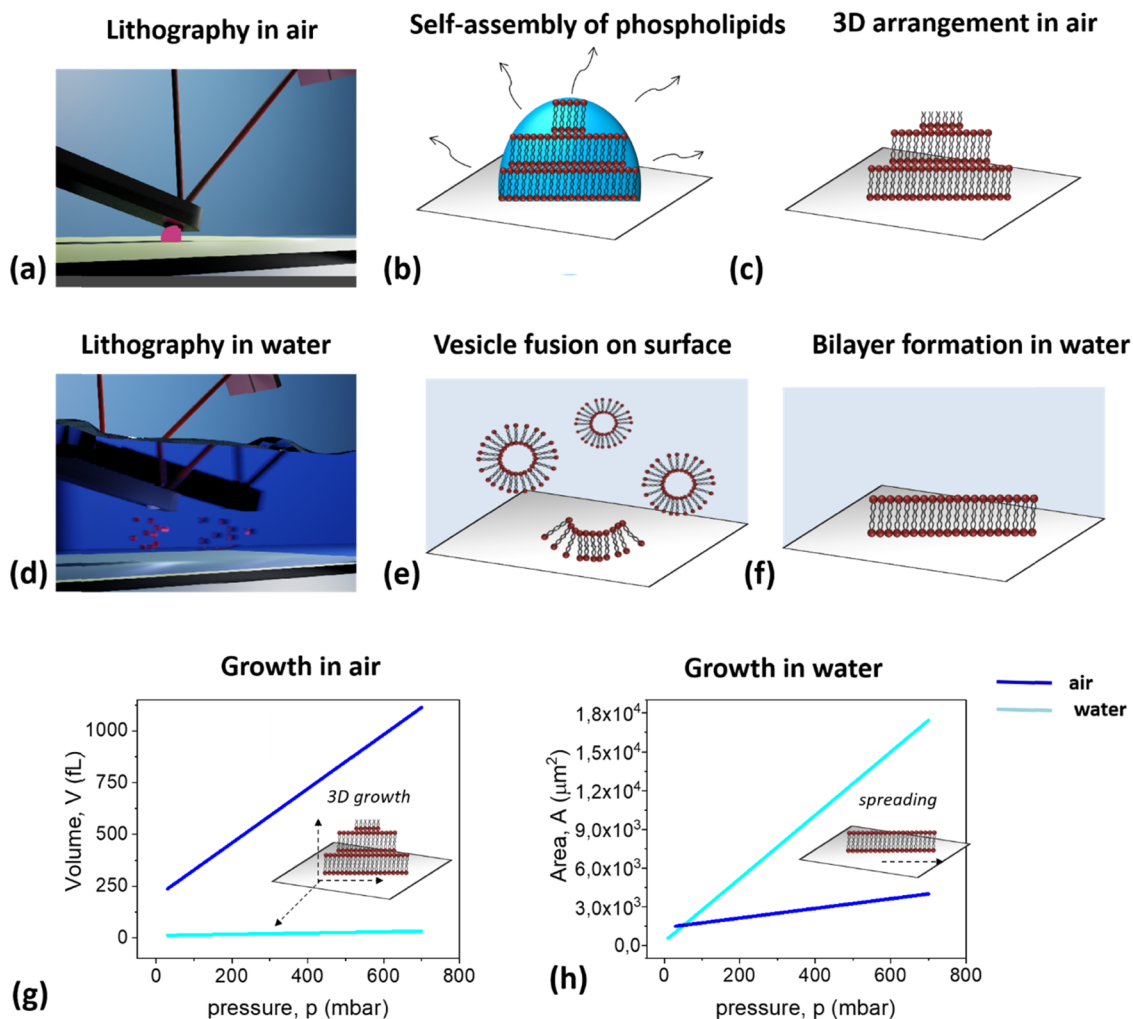
Figure 5. Routes for lipid patch patterning by FluidFM in air and in liquid. (a) Schematic setup for in air patterning. (b) In air, an ink droplet is deposited on the substrate, and the phospholipid molecules self assemble on the surface while the water in the ink evaporates, resulting in (c) ordered stacks of lipid membranes. (d) Schematic setup for in liquid patterning. (e) Here, vesicles released from the tip reach the surface and fuse to the substrate, resulting in (f) supported lipid bilayers. Fitted lines from experimental data obtained at a constant pulse length t = 500 ms show differences in (g) volume growth and (h) area growth as a function of the applied pressure. The inset shows sketches of the growth process in air and liquid environment.

vesicles fuse on the substrate (Figure 5e), forming a bilayer lipid membrane patch (Figure 5f).

When the lithography is carried out in air under the presented writing parameters, the output consists of a stack of lipids of a few hundreds of femtoliters in volume, with thicknesses of several tens of bilayers. The ink ejection from the nozzle is hampered by the liquid–air interface, which demands working at higher pressure values. The writing parameters can thus be tuned to obtain the desired feature size and control its three dimensional growth (Figure 5g).

In classical L DPN, the 3D structure of features stems from a layer by layer type deposition mode from a point like source in the form of the AFM tip.[21] In FluidFM, even when operating in air, the initial ink deposition is done as vesicles in aqueous carrier. In contrast to the FluidFM process in liquid, the water in the deposited ink droplet evaporates quickly, more and more condensing the remaining lipid component. The confinement imposed by the shrinking droplet hinders free spreading into a single SLB and forces the phospholipids to rearrange into the 3D stacks.

For a comparison between air and liquid lithography, the variations under changing pressure were studied since the size dependencies on this parameter display a linear behavior and a single regime in both cases. Linear fits to the experimental data obtained with a pulse length of t = 500 ms enable quantitative comparison of feature volumes and areas grown in air and liquid (Figure 5g,h). The slopes of the four lines are gathered in Table 2.

Table 2. Linear Fitted Slope Coefficients from Figure 5g,h

environment	volume growth [fL/mbar]	area growth [μm^2/mbar]
air	1.3	3.74
liquid	0.03	24.49

In air environment, all of the phospholipids ejected from the nozzle form the resulting lipid patch, whereas in liquid environment, an ink cloud ejected and only reaching the surface contributes to the feature formation. Therefore, the lower volume growth coefficient (0.03 fl/mbar in liquid vs to 1.3 fl/mbar in air) represents the loss of vesicles by diffusion

into the surrounding liquid media. In contrast, the unhindered spreading of the lipid bilayer in liquid leads to a considerably higher area growth coefficient (24.49 μm^2/mbar in liquid vs 3.74 μm^2/mbar in air).

4.2. Droplet Ejection for In-Air Printing. When operating the FluidFM in air, we have already shown that a different threshold pressure needs to be applied for the ink to produce a droplet in a way to allow printing. As mentioned before, this is related to the high resistance to expel a droplet originating from the liquid−air interface at the nozzle. Several authors have already addressed the problem of the production of a droplet on a microfluidic device and its ejection through a nozzle due to its relevance in several engineering applications, in particular micro printing technologies.[43,44] The behavior and printability of inks in inkjet printing can be predicted by considering a series of characteristic dimensionless numbers in fluid dynamics: the Reynolds (Re), Weber (We), and Ohnesorge (Oh) numbers. In particular, the Ohnesorge number is believed to be the most suitable measure for the formation of an ink droplet at a nozzle or aperture, as it relates the fluid inertia and viscous forces to the surface tension and is given by

$$Oh = \frac{\mu}{(\Upsilon \rho a)^{1/2}} \tag{1}$$

where μ is the viscosity, Υ is the surface tension, ρ is the ink density, and a is the drop diameter. Reis and Derby[45] established that to generate a droplet out of a nozzle, the fluid ink needs to be in the range

$$10 > Z > 1 \tag{2}$$

where

$$Z = 1/Oh \tag{3}$$

The ejection of a droplet depends, therefore, on the interplay between the mentioned ink physicochemical characteristics and the nozzle size. Importantly, the ink viscosity and surface tension (cohesive forces) are dependent on the molecular interactions; thus, the choice of the solvent is a critical step. Nevertheless, in the present case, to avoid damage or corrosion of the reservoir and microchannel (as part of tip construction will not withstand organic solvents), we have focused our study on water based inks.

The strong similarities between the in air operated FluidFM and inkjet printing technologies allow conducting an analogous study of the printing parameters. Duineveld et al.[46] suggested that, to overcome the hindering effects, the drop needs to have sufficient energy for drop ejection

$$v_{min} = \left(\frac{4\gamma}{\rho d} \right)^{1/2} \tag{4}$$

In our system, the ink velocity can be controlled by the applied pressure value. The velocity at threshold pressure is therefore related to the surface tension of the ink. To demonstrate one of the main assets of using the FluidFM for the fabrication of biomimetic membranes (patterning of phospholipid mixtures that cannot be processed by other soft lithography methods), we chose a biologically realistic lipid mixture (POPC/cholesterol/POPS in a relative composition of 60:20:20)[47,48] and compared it to dipalmitoylphosphatidylcholine (DPPC, also not writable in L DPN as it fluid gel transition temperature is beyond RT), pure DOPC, and DOPC +

1 oleoyl 2 (12 biotinyl(aminododecanoyl)) *sn* glycero 3 phos phoethanolamine (18:1−12:0 Biotin CAP PE) inks (as exam ples of standard L DPN inks) for threshold determinations. The obtained threshold values are compared to those of deionized water, and a water/glycerol (80:20 vol %) mixture, as used as a solvent in all of the lipid inks (Figure 3a). The addition of glycerol[49] to the mixtures is of utmost importance not only to avoid too quick evaporation of the ink but also to lower the cohesion forces and achieve ink printability. Keeping in mind that the droplet production out of a nozzle is determined by the interplay between the surface tension, ink viscosity, and droplet size, the relevant physical properties are gathered in Table 3 for the following discussion.

Table 3. Surface Tension and Viscosity Values at 20 °C

component	surface tension (20 °C) γ [mN/m]	viscosity (20 °C) μ [Pa s]
DI water	72	10^{-3}
glycerol[52]	63.4	1.412
DOPC[53,54]	0 15	∼0.240
DPPC[55,56]	0 70	
POPC[57,58]	0 45	∼0.260

As we see in the chart of Figure 3a, the water/glycerol mixture presents the highest threshold pressure of all. This value is significantly higher than the threshold value to expel a pure water drop out of the nozzle, and we believe that it is related to the change in viscosity that the addition of glycerol causes. On the other hand, the threshold pressure value for the DOPC vesicle ink is the lowest, while all of the other inks present similar values in the range between 100 and 200 mbar. A plausible explanation to this is to consider a direct correlation between the threshold pressure of the ink and its surface tension, as lipids—and in particular, DOPC—are known to lower the water surface tension acting as a surfactant between the water and air interface (see Figure 3b). It is important to point out here that the chosen concentration of phospholipids is quite high, namely, 2 orders of magnitude above the critical micelle concentration, which is estimated to be 50 μM at room temperature, in the case of DOPC.[50,51]

The viscosity, on the other hand, plays a minor role in the phospholipid containing inks, as the content of phospholipids is high enough to alter the ink surface tension and simultaneously too low to produce significant changes in the viscosity of the water/glycerol mixture.

4.3. Lipid Flow in Air and Water. Our experiments have so far evidenced that the ink flow is linearly dependent on the writing parameters. This linear behavior of the flow versus increasing pressure values was reported by Zambelli et al.[59] for FluidFM deposition in liquid environment, setting an analogy to an electrical circuit, with

$$Q = \Delta p / R \tag{5}$$

where Q is the ink flow, Δp is the applied pressure, and R is the hydrodynamic resistance of the microchannel. This model can also be extrapolated to air environment, although a much higher resistance is expected due to the additional influence of the liquid−air interface that hinders the drop formation at the cantilever aperture, as discussed in the previous section. It is important to remark here that deviations from this linear behavior have been observed at high applied pressures (as we pointed out in Figure 3c).

Unlike in air environment, where a threshold pressure related to the surface tension of the ink is needed to be overcome for deposition to start, in liquid environment, the ink flow through the microchannel is only hampered by the hydrodynamic resistance of the cantilever microchannel,[59] namely

$$R_{\mathrm{h}} = \frac{12\mu l_{\mathrm{c}}}{w_{\mathrm{c}}\, h_{\mathrm{c}}^{3}\left(1-0.63\frac{h_{\mathrm{c}}}{w_{\mathrm{c}}}\right)} \tag{6}$$

This value depends solely on the cantilever dimensions (width w_{c}, height h_{c}, and length l_{c}), and the viscosity of the ink (μ).

Because the hydrodynamic resistance is considerably lower than the resistance arising as a result of the ink surface tension in air media, lipid patterns can be written with much lower applied pressure.

5. CONCLUSIONS

While a variety of soft lithography methods and scanning probe lithography methods can be used to fabricate supported lipid membranes in arrays and multiplexed manner with a very high accuracy and features next to each other in close vicinity, these methods all inherently struggle to create biomimetic membranes of complex natural composition. In this work, we have demonstrated the feasibility of using the FluidFM technology as a tool to direct write biomimetic membranes in air and in aqueous media and simultaneously studied the relevant parameters to the feature fabrication, as well as the governing mechanism. A comparative study has shown that while in air operated FluidFM enables us to grow 3D lipid patches, similar to other soft lithography techniques, in liquid operated FluidFM yields single phospholipid bilayers, which tend to spread on the surface. By the use of vesicle based inks, FluidFM opens up the route to directly incorporate membrane proteins during the writing process consistently providing physiological conditions. We demonstrated that it is possible to enlarge the number of components that can be added to a membrane, compared to other lithography techniques. An important example is the successfully achieved incorporation of cholesterol, as biological membranes are composed of up to 40% cholesterol, which dramatically changes its mechanical properties and thus results in relevant changes in its functionality and the writing of physiological lipid cholesterol mixture of POPC/cholesterol/POPS. If the highest resolution is required, two methods for patterning very small features have been explored in air and liquid media. The implementation of direct in liquid patterning of multiplexed and complex biomimetic lipid membrane stack arrays will enable many future applications in biological and biomedical experiments, where these arrays can act as sophisticated, highly realistic model membranes in interaction and screening applications as well as bioactive interfaces for cell culture.

■ ASSOCIATED CONTENT

● Supporting Information

The Supporting Information is available free of charge at https://pubs.acs.org/doi/10.1021/acsami.1c15166.

Printing small features; determination of an ink threshold pressure value in air; influence of substrate hydrophilicity; feature shape after in air lithography; AFM imaging in liquid; patterning in different research environments; and air bubble assisted printing of small features in liquid (PDF)

■ AUTHOR INFORMATION

Corresponding Author

Eider Berganza − *Institute of Nanotechnology (INT) & Karlsruhe Nano Micro Facility (KNMF), Karlsruhe Institute of Technology (KIT), 76344 Eggenstein Leopoldshafen, Germany;* ⊙ orcid.org/0000 0002 0114 4925; Email: eider.eguiarte@kit.edu

Author

Michael Hirtz − *Institute of Nanotechnology (INT) & Karlsruhe Nano Micro Facility (KNMF), Karlsruhe Institute of Technology (KIT), 76344 Eggenstein Leopoldshafen, Germany;* ⊙ orcid.org/0000 0002 2647 5317

Author Contributions

The manuscript was written through contributions of all authors.

Notes

The authors declare no competing financial interest.

■ ABBREVIATIONS

AFM, atomic force microscopy
BSA, bovine serum albumin
DI, dionized water
DNA, deoxyribonucleic acid
DPN, dip pen nanolithography
DOPC, 1,2 dioleoyl *sn* glycero 3 phosphocholine
DPPC, dipalmitoylphosphatidylcholine
FluidFM, fluid force microscopy
μCP, microchannel cantilever spotting
Oh, Ohnesorge
PBS, phosphate buffered saline
POPC, 1 palmitoyl 2 oleoyl *sn* glycero 3 phospho L serine
PPL, polymer pen lithography
Re, Reynolds
RT, room temperature
SPL, scanning probe lithography
SLB, supported lipid membranes
We, Weber

■ REFERENCES

(1) Nair, P. M.; Salaita, K.; Petit, R. S.; Groves, J. T. Using patterned supported lipid membranes to investigate the role of receptor organization in intercellular signaling. *Nat. Protoc.* **2011**, *6*, 523−39.
(2) Glazier, R.; Salaita, K. Supported lipid bilayer platforms to probe cell mechanobiology. *Biochim. Biophys. Acta, Biomembr.* **2017**, *1859*, 1465−82.

(3) Arrabito, G.; Ferrara, V.; Bonasera, A.; Pignataro, B. Artificial Biosystems by Printing Biology. *Small* **2020**, *16*, No. 1907691.

(4) Lowry, T. W.; Hariri, H.; Prommapan, P.; Kusi Appiah, A.; Vafai, N.; Bienkiewicz, E. A.; Van Winkle, D. H.; Stagg, S. M.; Lenhert, S. Quantification of Protein Induced Membrane Remodeling Kinetics In Vitro with Lipid Multilayer Gratings. *Small* **2016**, *12*, 506−15.

(5) Su, H.; Liu, H. Y.; Pappa, A. M.; Hidalgo, T. C.; Cavassin, P.; Inal, S.; Owens, R. M.; Daniel, S. Facile Generation of Biomimetic Supported Lipid Bilayers on Conducting Polymer Surfaces for Membrane Biosensing. *ACS Appl. Mater. Interfaces* **2019**, *11*, 43799−810.

(6) Heath, G. R.; Li, M.; Rong, H.; Radu, V.; Frielingsdorf, S.; Lenz, O.; Butt, J. N.; Jeuken, L. J. C. Multilayered Lipid Membrane Stacks for Biocatalysis Using Membrane Enzymes. *Adv. Funct. Mater.* **2017**, *27*, No. 1606265.

(7) Kawan, M.; Hidalgo, T. C.; Du, W.; Pappa, A. M.; Owens, R. M.; McCulloch, I.; Inal, S. Monitoring supported lipid bilayers with n type organic electrochemical transistors Mater. *Horizons* **2020**, *7*, 2348−58.

(8) Hirtz, M.; Sekula Neuner, S.; Urtizberea, A.; Fuchs, H. *Functional Lipid Assemblies by Dip Pen Nanolithography and Polymer Pen Lithography Soft Matter Nanotechnology: From Structure to Function*; Wiley VCH: Weinheim, 2015; pp 161−186.

(9) Kusi Appiah, A. E.; Vafai, N.; Cranfill, P. J.; Davidson, M. W.; Lenhert, S. Lipid multilayer microarrays for in vitro liposomal drug delivery and screening. *Biomaterials* **2012**, *33*, 4187−94.

(10) Wu, N.; Chen, F.; Zhao, Y.; Yu, X.; Wei, J.; Zhao, Y. Functional and Biomimetic DNA Nanostructures on Lipid Membranes. *Langmuir* **2018**, *34*, 14721−14730.

(11) Liu, H. Y.; Kumar, R.; Zhong, C.; Gorji, S.; Paniushkina, L.; Masood, R.; Wittel, U. A.; Fuchs, H.; Nazarenko, I.; Hirtz, M. Rapid Capture of Cancer Extracellular Vesicles by Lipid Patch Microarrays. *Adv. Mater.* **2021**, *33*, No. 2008493.

(12) Siontorou, C. G.; Nikoleli, G. P.; Nikolelis, D. P.; Karapetis, S. K. Artificial lipid membranes: Past, present, and future. *Membranes* **2017**, *7*, No. 38.

(13) Andersson, J.; Köper, I. Tethered and Polymer Supported Bilayer Lipid Membranes: Structure and Function. *Membranes* **2016**, *6*, 30.

(14) van Weerd, J.; Karperien, M.; Jonkheijm, P. Supported Lipid Bilayers for the Generation of Dynamic Cell Material Interfaces. *Adv. Healthcare Mater.* **2015**, *4*, 2743−79.

(15) Kang, M.; Tuteja, M.; Centrone, A.; Topgaard, D.; Leal, C. Nanostructured Lipid Based Films for Substrate Mediated Applica tions in Biotechnology. *Adv. Funct. Mater.* **2018**, *28*, No. 1704356.

(16) Théry, C.; Witwer, K. W.; Aikawa, E.; Alcaraz, M. J.; Anderson, J. D.; Andriantsitohaina, R.; Antoniou, A.; Arab, T.; Archer, F.; Atkin Smith, G. K.; Ayre, D. C.; Bach, J. M.; Bachurski, D.; Baharvand, H.; Balaj, L.; Baldacchino, S.; Bauer, N. N.; Baxter, A. A.; Bebawy, M.; Beckham, C.; Bedina Zavec, A.; Benmoussa, A.; Berardi, A. C.; Bergese, P.; Bielska, E.; Blenkiron, C.; Bobis Wozowicz, S.; Boilard, E.; Boireau, W.; Bongiovanni, A.; Borràs, F. E.; Bosch, S.; Boulanger, C. M.; Breakefield, X.; Breglio, A. M.; Brennan, M. Á.; Brigstock, D. R.; Brisson, A.; Broekman, M. L. D.; Bromberg, J. F.; Bryl Górecka, P.; Buch, S.; Buck, A. H.; Burger, D.; Busatto, S.; Buschmann, D.; Bussolati, B.; Buzás, E. I.; Byrd, J. B.; Camussi, G.; Carter, D. R. F.; Caruso, S.; Chamley, L. W.; Chang, Y. T.; Chen, C.; Chen, S.; Cheng, L.; Chin, A. R.; Clayton, A.; Clerici, S. P.; Cocks, A.; Cocucci, E.; Coffey, R. J.; Cordeiro da Silva, A.; Couch, Y.; Coumans, F. A. W.; Coyle, B.; Crescitelli, R.; Criado, M. F.; D'Souza Schorey, C.; Das, S.; Datta Chaudhuri, A.; de Candia, P.; De Santana, E. F.; De Wever, O.; del Portillo, H. A.; Demaret, T.; Deville, S.; Devitt, A.; Dhondt, B.; Di Vizio, D.; Dieterich, L. C.; Dolo, V.; Dominguez Rubio, A. P.; Dominici, M.; Dourado, M. R.; Driedonks, T. A. P.; Duarte, F. V.; Duncan, H. M.; Eichenberger, R. M.; Ekström, K.; EL Andaloussi, S.; Elie Caille, C.; Erdbrügger, U.; Falcón Pérez, J. M.; Fatima, F.; Fish, J. E.; Flores Bellver, M. Minimal information for studies of extracellular vesicles 2018 (MISEV2018): a position statement of the International Society for Extracellular Vesicles and update of the MISEV2014 guidelines. *J. Extracell. Vesicles* **2018**, *7*, No. 1535750.

(17) Yáñez Mó, M.; Siljander, P. R. M.; Andreu, Z.; Bedina Zavec, A.; Borràs, F. E.; Buzas, E. I.; Buzas, K.; Casal, E.; Cappello, F.; Carvalho, J.; Colás, E.; Cordeiro da Silva, A.; Fais, S.; Falcon Perez, J. M.; Ghobrial, I. M.; Giebel, B.; Gimona, M.; Graner, M.; Gursel, I.; Gursel, M.; Heegaard, N. H. H.; Hendrix, A.; Kierulf, P.; Kokubun, K.; Kosanovic, M.; Kralj Iglic, V.; Krämer Albers, E. M.; Laitinen, S.; Lässer, C.; Lener, T.; Ligeti, E.; Line, A.; Lipps, G.; Llorente, A.; Lötvall, J.; Manček Keber, M.; Marcilla, A.; Mittelbrunn, M.; Nazarenko, I.; Nolte 't Hoen, E. N. M.; Nyman, T. A.; O'Driscoll, L.; Olivan, M.; Oliveira, C.; Pállinger, É.; del Portillo, H. A.; Reventós, J.; Rigau, M.; Rohde, E.; Sammar, M.; Sánchez Madrid, F.; Santarém, N.; Schallmoser, K.; Stampe Ostenfeld, M.; Stoorvogel, W.; Stukelj, R.; Van der Grein, S. G.; Vasconcelos, H.; Wauben, M. H. M.; De Wever, O. Biological properties of extracellular vesicles and their physiological functions. *J. Extracell. Vesicles* **2015**, *4*, 27066.

(18) Harding, C. V.; Heuser, J. E.; Stahl, P. D. Exosomes: Looking back three decades and into the future. *J. Cell Biol.* **2013**, *200*, 367−71.

(19) Serdiuk, T.; Mari, S. A.; Müller, D. J. Pull and Paste of Single Transmembrane Proteins. *Nano Lett.* **2017**, *17*, 4478−88.

(20) Zieleniecki, J. L.; Nagarajan, Y.; Waters, S.; Rongala, J.; Thompson; Hrmova, M.; Köper, I. Cell Free Synthesis of a Functional Membrane Transporter into a Tethered Bilayer Lipid Membrane. *Langmuir* **2016**, *32*, 2445−9.

(21) Lenhert, S.; Sun, P.; Wang, Y.; Fuchs, H.; Mirkin, C. A. Massively parallel dip pen nanolithography of heterogeneous supported phospholipid multilayer patterns. *Small* **2007**, *3*, 71−5.

(22) Ainla, A.; Gözen, I.; Hakonen, B.; Jesorka, A. Lab on a Biomembrane: rapid prototyping and manipulation of 2D fluidic lipid bilayers circuits. *Sci. Rep.* **2013**, *3*, No. 2743.

(23) Sekula Neuner, S.; de Freitas, M.; Tröster, L. M.; Jochum, T.; Levkin, P. A.; Hirtz, M.; Fuchs, H. Phospholipid arrays on porous polymer coatings generated by micro contact spotting. *Beilstein J. Nanotechnol.* **2017**, *8*, 715−22.

(24) Hovis, J. S.; Boxer, S. G. Patterning and composition arrays of supported lipid bilayers by microcontact printing. *Langmuir* **2001**, *17*, 3400−5.

(25) Brinkmann, F.; Hirtz, M.; Greiner, A. M.; Weschenfelder, M.; Waterkotte, B.; Bastmeyer, M.; Fuchs, H. Interdigitated Multicolored Bioink Micropatterns by Multiplexed Polymer Pen Lithography. *Small* **2013**, *9*, 3266−3275.

(26) Urtizberea, A.; Hirtz, M. A diffusive ink transport model for lipid dip pen nanolithography. *Nanoscale* **2015**, *7*, 15618−34.

(27) Sekula, S.; Fuchs, J.; Weg Remers, S.; Nagel, P.; Schuppler, S.; Fragala, J.; Theilacker, N.; Franzreb, M.; Wingren, C.; Ellmark, P.; Borrebaeck, C. A. K.; Mirkin, C. A.; Fuchs, H.; Lenhert, S. Multiplexed lipid dip pen nanolithography on subcellular scales for the templating of functional proteins and cell culture. *Small* **2008**, *4*, 1785−93.

(28) Lenhert, S.; Mirkin, C. A.; Fuchs, H. In situ lipid dip pen nanolithography under water. *Scanning* **2010**, *32*, 15−23.

(29) Hirtz, M.; Oikonomou, A.; Georgiou, T.; Fuchs, H.; Vijayaraghavan, A. Multiplexed biomimetic lipid membranes on graphene by dip pen nanolithography. *Nat. Commun.* **2013**, *4*, No. 2591.

(30) Willems, N.; Urtizberea, A.; Verre, A. F.; Iliut, M.; Lelimousin, M.; Hirtz, M.; Vijayaraghavan, A.; Sansom, M. S. P. Biomimetic Phospholipid Membrane Organization on Graphene and Graphene Oxide Surfaces: A Molecular Dynamics Simulation Study. *ACS Nano* **2017**, *11*, 1613−25.

(31) Berganza, E.; Ebrahimkutty, M. P.; Vasantham, S. K.; Zhong, C.; Wunsch, A.; Navarrete, A.; Galic, M.; Hirtz, M. A multiplexed phospholipid membrane platform for curvature sensitive protein screening. *Nanoscale* **2021**, *13*, 12642−12650.

(32) Navikas, V.; Gavutis, M.; Rakickas, T.; Valiokas, R. Scanning Probe Directed Assembly and Rapid Chemical Writing Using

Nanoscopic Flow of Phospholipids. *ACS Appl. Mater. Interfaces* **2019**, *11*, 28449−60.

(33) Kumar, R.; Urtizberea, A.; Ghosh, S.; Bog, U.; Rainer, Q.; Lenhert, S.; Fuchs, H.; Hirtz, M. Polymer Pen Lithography with Lipids for Large Area Gradient Patterns. *Langmuir* **2017**, *33*, 8739−48.

(34) Meister, A.; Gabi, M.; Behr, P.; Studer, P.; Vörös, J.; Niedermann, P.; Bitterli, J.; Polesel Maris, J.; Liley, M.; Heinzelmann, H.; Zambelli, T. FluidFM: Combining atomic force microscopy and nanofluidics in a universal liquid delivery system for single cell applications and beyond. *Nano Lett.* **2009**, *9*, 2501−7.

(35) Grüter, R. R.; Vörös, J.; Zambelli, T. FluidFM as a lithography tool in liquid: Spatially controlled deposition of fluorescent nano particles. *Nanoscale* **2013**, *5*, 1097−104.

(36) Saha, P.; Duanis Assaf, T.; Reches, M. Fundamentals and Applications of FluidFM Technology in Single Cell Studies. *Adv. Mater. Interfaces* **2020**, *7*, No. 2001115.

(37) Guillaume Gentil, O.; Potthoff, E.; Ossola, D.; Dörig, P.; Zambelli, T.; Vorholt, J. A. Force Controlled Fluidic Injection into Single Cell Nuclei. *Small* **2012**, *9*, 1904−1907.

(38) Hirt, L.; Grüter, R. R.; Berthelot, T.; Cornut, R.; Vörös, J.; Zambelli, T. Local surface modification via confined electrochemical deposition with FluidFM. *RSC Adv.* **2015**, *5*, 84517−22.

(39) Reeves, J. P.; Dowben, R. M. Formation and properties of thin walled phospholipid vesicles. *J. Cell. Physiol.* **1969**, *73*, 49−60.

(40) Horn, R. G. Direct measurement of the force between two lipid bilayers and observation of their fusion. *Biochim. Biophys. Acta, Biomembr.* **1984**, *778*, 224−228.

(41) Attwood, S. J.; Choi, Y.; Leonenko, Z. Preparation of DOPC and DPPC Supported Planar Lipid Bilayers for Atomic Force Microscopy and Atomic Force Spectroscopy. *Int. J. Mol. Sci.* **2013**, *14*, 3514−3539.

(42) Barenholz, Y.; Gibbes, D.; Litman, B. J.; Goll, J.; Thompson, T. E.; Carlson, F. D. A simple method for the preparation of homogeneous phospholipid vesicles. *Biochemistry* **1977**, *16*, 2806−10.

(43) Modak, C. D.; Kumar, A.; Tripathy, A.; Sen, P. Drop impact printing. *Nat. Commun.* **2020**, *11*, No. 4327.

(44) Morita, A.; Carastan, D.; Demarquette, N. Influence of drop volume on surface tension evaluated using the pendant drop method. *Colloid Polym. Sci.* **2002**, *280*, 857−64.

(45) Reis, N.; Derby, B. Ink Jet Deposition of Ceramic Suspensions: Modeling and Experiments of Droplet Formation. *MRS Proc.* **2000**, *625*, No. 117.

(46) Duineveld, P. C.; de Kok, M. M.; Buechel, M.; Sempel, A.; Mutsaers, K. A. H.; van de Weijer, P.; Camps, I. G. J.; van de Biggelaar, T.; Rubingh, J. E. J. M.; Haskal, E. I. Ink Jet Printing of Polymer Light emitting Devices. In *Proceedings of the SPIE Conference, Organic Light Emitting Materials and Devices*, San Diego, CA, 2002.

(47) Drücker, P.; Pejic, M.; Grill, D.; Galla, H. J.; Gerke, V. Cooperative Binding of Annexin A2 to Cholesterol and Phosphati dylinositol 4,5 Bisphosphate Containing Bilayers. *Biophys. J.* **2014**, *107*, 2070−81.

(48) Drücker, P.; Grill, D.; Gerke, V.; Galla, H. J. Formation and Characterization of Supported Lipid Bilayers Containing Phosphati dylinositol 4,5 bisphosphate and Cholesterol as Functional Surfaces. *Langmuir* **2014**, *30*, 14877−86.

(49) Mallinson, S. G.; McBain, G. D.; Horrocks, G. D. Viscosity and Surface Tension Of Aqueous Mixtures. In *Proceedings of the 20th Australasian Fluid Mechanics Conference*; AFMC: Perth, Australia, 2016.

(50) Pohl, H.; Morgner, H. Behavior of 1,2 dioleoyl sn glycero 3 phosphocholine at the surface of 3 hydroxypropionitrile near the critical micelle concentration. *J. Phys. Chem. B* **2010**, *114*, 12847−50.

(51) Cui, L.; Kittipongpittaya, K.; McClements, D. J.; Decker, E. A. Impact of Phosphoethanolamine Reverse Micelles on Lipid Oxidation in Bulk Oils. *J. Am. Oil Chem. Soc.* **2014**, *91*, 1931−7.

(52) Takamura, K.; Fischer, H.; Morrow, N. R. Physical properties of aqueous glycerol solutions. *J. Pet. Sci. Eng.* **2012**, *98−99*, 50−60.

(53) Reddy, A. S.; Warshaviak, D. T.; Chachisvilis, M. Effect of membrane tension on the physical properties of DOPC lipid bilayer membrane. *Biochim. Biophys. Acta, Biomembr.* **2012**, *1818*, 2271−81.

(54) Smith, R. D.; Berg, J. C. The collapse of surfactant monolayers at the air—water interface. *J. Colloid Interface Sci.* **1980**, *74*, 273−86.

(55) McConnell, H. M. Structures and Transitions in Lipid Monolayers at the Air Water Interface. *Annu. Rev. Phys. Chem.* **1991**, *42*, 171−95.

(56) Olżyńska, A.; Zubek, M.; Roeselova, M.; Korchowiec, J.; Cwiklik, L. Mixed DPPC/POPC Monolayers: All atom Molecular Dynamics Simulations and Langmuir Monolayer Experiments. *Biochim. Biophys. Acta, Biomembr.* **2016**, *1858*, 3120−30.

(57) Wu, Y.; Štefl, M.; Olzyńska, A.; Hof, M.; Yahioglu, G.; Yip, P.; Casey, D. R.; Ces, O.; Humpolíčková, J.; Kuimova, M. K. Molecular rheometry: direct determination of viscosity in Lo and Ld lipid phases via fluorescence lifetime imaging. *Phys. Chem. Chem. Phys.* **2013**, *15*, 14986.

(58) Wnętrzak, A.; Łątka, K.; Dynarowicz Łątka, P. Interactions of Alkylphosphocholines with Model Membranes—The Langmuir Monolayer Study. *J. Membr. Biol.* **2013**, *246*, 453−66.

(59) Zambelli, T.; Aebersold, M.; Behr, P.; Han, H.; Hirt, L.; Guillaume Gentil, O.; Vörös, J. FluidFM: Development of the Instrument as well as Its Applications for 2D and 3D Lithography. Open Space Microfluidics. *Open Space Microfluid.* **2018**, *295−322*.